Functional redundancy between the XLF and DNA-PKcs DNA repair factors in V(D)J recombination and nonhomologous DNA end joining

Valentyn Oksenych[a,b,c], Vipul Kumar[a,b,c], Xiangyu Liu[d], Chunguang Guo[a,b,c], Bjoern Schwer[a,b,c], Shan Zha[d], and Frederick W. Alt[a,b,c,1]

[a]Howard Hughes Medical Institute, [b]Program in Cellular and Molecular Medicine, Boston Children's Hospital, and [c]Department of Genetics, Harvard Medical School, Boston, MA 02115; and [d]Institute for Cancer Genetics, Department of Pathology and Cell Biology and Department of Pediatrics, College of Physicians and Surgeons, Columbia University, New York, NY 10032

Contributed by Frederick W. Alt, December 26, 2012 (sent for review December 18, 2012)

Classical nonhomologous end joining (C-NHEJ) is a major mammalian DNA double-strand break (DSB) repair pathway that is required for assembly of antigen receptor variable region gene segments by V(D)J recombination. Recombination activating gene endonuclease initiates V(D)J recombination by generating DSBs between two V(D)J coding gene segments and flanking recombination signal sequences (RS), with the two coding ends and two RS ends joined by C-NHEJ to form coding joins and signal joins, respectively. During C-NHEJ, recombination activating gene factor generates two coding ends as covalently sealed hairpins and RS ends as blunt 5′-phosphorylated DSBs. Opening and processing of coding end hairpins before joining by C-NHEJ requires the DNA-dependent protein kinase catalytic subunit (DNA-PKcs). However, C-NHEJ of RS ends, which do not require processing, occurs relatively normally in the absence of DNA-PKcs. The XRCC4-like factor (XLF) is a C-NHEJ component that is not required for C-NHEJ of chromosomal signal joins or coding joins because of functional redundancy with ataxia telangiectasia mutated kinase, a protein that also has some functional overlap with DNA-PKcs in this process. Here, we show that XLF has dramatic functional redundancy with DNA-PKcs in the V(D)J SJ joining process, which is nearly abrogated in their combined absence. Moreover, we show that XLF functionally overlaps with DNA-PKcs in normal mouse development, promotion of genomic stability in mouse fibroblasts, and in IgH class switch recombination in mature B cells. Our findings suggest that DNA-PKcs has fundamental roles in C-NHEJ processes beyond end processing that have been masked by functional overlaps with XLF.

Cernunnos | nej1 | nhej1 | SCID | T-FISH

Double-strand break (DSB) repair is crucial for maintaining stability of the mammalian genome. There are two major DNA DSB repair pathways in mammalian cells. Homologous recombination repairs DSBs with high fidelity and is active in the S/G2 phases of the cell cycle. Classical nonhomologous end joining (C-NHEJ) rejoins DSBs, often imprecisely, throughout the cell cycle (1, 2). During C-NHEJ, the Ku70/Ku80 heterodimer (Ku) recognizes the DSB and recruits the DNA-dependent protein kinase catalytic subunit (DNA-PKcs) to form a DNA-dependent protein kinase holoenzyme (DNA-PK). DNA-PK activates the Artemis endonuclease, which can contribute to the processing of DSB ends, if necessary, to allow their ligation (3). Ku70/Ku80 also recruits the XRCC4/DNA ligase 4 (Lig4) complex that ligates DSB ends. Ku70, Ku80, XRCC4, and Lig4 are considered to be "core" C-NHEJ factors because they are required to repair all types of DSB ends. However, deficiency for Ku70, Ku80, XRCC4, Lig4, Artemis, or DNA-PKcs abrogates lymphocyte development and leads to severe combined immunodeficiency (SCID) in mice due to their requisite role in coding join (CJ) formation (1).

During the B and T lymphocyte development, exons that encode Ig (Ig) and T-cell receptor variable regions are assembled from V, D, and J gene segments. This V(D)J recombination process is initiated by the RAG1/RAG2 (RAG) endonuclease (4). V, D, and J coding segments are each flanked by RSs that target RAG. RAG cleaves between the borders of two appropriately paired coding segments and their flanking recombination signal sequences (RSs) to generate two hairpin-sealed coding ends (CEs) and two blunt 5′-phosphorylated RS ends (SEs). The SEs are ligated back together without further processing, whereas the coding ends must be opened and processed before they can be joined. Both CE and SE are joined by C-NHEJ pathway. In this context, Ku and the XRCC4/Lig4 complex are required for both CJ and signal joins (SJ) formation. However, although DNA-PKcs and Artemis are absolutely required for CJ formation due to their role in opening and processing these ends, RS join formation can occur in their absence as these ends do not require further processing (1, 2, 4). IgH class switch recombination (CSR) is a second type of programmed genome rearrangement that occurs in activated mature B cells to allow expression of different classes of antibodies. CSR is initiated by activation-induced cytidine deaminase, the activity of which results in DSBs in large switch (S) regions flanking different sets of IgH constant region exons. These DSBs are joined between two different S regions by C-NHEJ, or in the absence of C-NHEJ, at reduced levels by alternative end-joining pathways (1). DNA-PKcs is required for fully normal CSR (5–9).

DNA-PKcs mutations in mice lead to severe combined immune deficiency due to inability to form V(D)J CJs (10–12). Both point mutations in the kinase domain of DNA-PKcs (SCID mice) and elimination of DNA-PKcs expression by gene-targeted mutation abrogate CJ formation (13–15). However, in the absence of DNA-PKcs, SJ formation occurs at near normal levels in embryonic stem cells and pro-B cells (15, 16), but occurs at reduced levels with decreased fidelity in various nonlymphoid cells (17–19). During V(D)J recombination, DSBs activate ataxia telangiectasia mutated (ATM) kinase (4). ATM belongs to the same family of protein kinases as DNA-PKcs; and, indeed, these two kinases have common substrates (i.e., histone H2AX). ATM is required for fully normal chromosomal CJ formation, but it is dispensable for SJ formation (20). Combined deficiency for ATM and DNA-PKcs in mice leads to embryonic lethality (21, 22). Moreover, ATM and DNA-PKcs have redundant functions in SE joining in pro-B cells (16, 23). When both proteins are inactivated, or when ATM-deficient and DNA-PKcs-deficient pro-B cells are treated with DNA-PKcs and ATM specific inhibitors, respectively, SE joining is greatly impaired (16, 23). ATM and DNA-PKcs also have redundant functions in CSR, as switching to IgG1 and IgG3 was

Author contributions: V.O., V.K., X.L., C.G., B.S., S.Z., and F.W.A. designed research; V.O., V.K., X.L., C.G., B.S., and S.Z. performed research; V.O. and C.G. contributed new reagents/analytic tools; V.O., V.K., X.L., C.G., B.S., S.Z., and F.W.A. analyzed data; and V.O. and F.W.A. wrote the paper.

The authors declare no conflict of interest.

Freely available online through the PNAS open access option.

[1]To whom correspondence should be addressed. E-mail: alt@enders.tch.harvard.edu.

This article contains supporting information online at www.pnas.org/lookup/suppl/doi:10.1073/pnas.1222573110/-/DCSupplemental.

reduced in ATM-deficient B cells when treated with DNA-PKcs inhibitors (8).

The XRCC4-like factor (XLF; also called Cernunnos in humans, or nej1 in yeast) is a C-NHEJ factor that is recruited by Ku (24) and has structural relatedness to and interacts with XRCC4 (25). Human XLF deficiency leads to immunodeficiency and developmental defects (26, 27). Correspondingly, embryonic stem cells and fibroblasts from XLF-deficient mice have ionizing radiation sensitivity, genomic instability, and impaired extrachromosomal V(D)J recombination (28). In addition, CSR is reduced in XLF-deficient mouse B cells (29). However, chromosomal V(D)J recombination is largely normal in developing lymphocytes and pro-B-cell lines from XLF-deficient mice (29, 30) because of XLF functional redundancy with ATM and downstream substrates, including H2AX and 53BP1 in C-NHEJ (31–33). Thus, XLF/ATM and XLF/53BP1 double-deficient mice are smaller than single-deficient littermates, have a SCID phenotype associated with severely deficient V(D)J CE and SE joining, and have a greater reduction in CSR than single-deficient mice (31–33). XLF/H2AX double-deficient pro-B lines also have severely impaired chromosomal V(D)J recombination (31). In addition, unjoined CEs and SEs generated during attempted V(D)J recombination in XLF/H2AX and XLF/53BP1 double-deficient pro-B cells are highly resected, consistent with a role for H2AX and 53BP1 in end protection (34–36). It is notable that ATM deficiency or treatment with ATM inhibitors rescues the end resection, but not the V(D)J joining phenotype of XLF/H2AX or XLF/53BP1 double-deficient pro-B lines (31, 32); this is consistent with ATM having both a role in end joining and in activating the CtIP nuclease for end resection (34). Potential roles for XLF in end protection have been speculated but not tested.

Results

Combined Deficiency of DNA-PKcs and XLF Affects Mouse Growth and Viability. Mice with combined deficiency of DNA-PKcs and XLF ($XLF^{\Delta/\Delta}DNA\text{-}PKcs^{-/-}$) were obtained from breeding mice heterozygous for DNA-PKcs and homozygous for an XLF null allele ($XLF^{\Delta/\Delta}DNA\text{-}PKcs^{+/-}$). $XLF^{\Delta/\Delta}DNA\text{-}PKcs^{-/-}$ embryos occurred at approximately expected ratios at E15.5 (Fig. 1*A*), showing that the double-deficient genotype does not result in early embryonic lethality. However, $XLF^{\Delta/\Delta}DNA\text{-}PKcs^{-/-}$ mice appeared to be born at sub-Mendelian ratios and few survived past P7 (Fig. 1*A*) and none of the ones survived past day P10. Live-born $XLF^{\Delta/\Delta}DNA\text{-}PKcs^{-/-}$ pups were significantly smaller than their littermates (Fig. 1*B*). Mice with combined deficiency of Artemis and XLF ($XLF^{\Delta/\Delta}Artemis^{-/-}$) were obtained from breeding mice heterozygous for Artemis and homozygous for an XLF null allele ($XLF^{\Delta/\Delta}Artemis^{+/-}$). These mice were born at Mendelian ratios (Fig. 1*A*) and had no obvious defects beyond expected V(D)J recombination or genomic stability phenotypes associated with one or the other single-deficient genotype (see below). We conclude that XLF and DNA-PKcs have redundant functions in mouse development, reminiscent of those associated with core C-NHEJ deficiencies, and which, correspondingly, are not related to the role of DNA-PKcs in activating Artemis.

DNA-PKcs kKinase Activity Is Required for V(D)J SJ Formation in XLF-Deficient Pro-B Lines. Single deficiency for XLF or DNA-PKcs does not lead to major defects in SE joining during chromosomal V(D)J recombination in pro–B-cell lines (16, 31, 32) (Fig. 2 *A*–*C*). However, double deficiency for XLF and ATM markedly impaired SE joining (31). As DNA-PKcs and ATM belong to the same family of protein kinases, we tested whether XLF has functional redundancy with DNA-PKcs. For this, we generated WT, $XLF^{\Delta/\Delta}$, $DNA\text{-}PKcs^{-/-}$, or $XLF^{\Delta/\Delta}DNA\text{-}PKcs^{-/-}$ v-Abl kinase transformed (v-Abl) pro-B cells harboring a *bcl-2* transgene. We treated the cells with the v-Abl kinase inhibitor STI571 to arrest the cells in the G1 cell-cycle phase leading to induction of RAG expression and V(D)J recombination. In these experiments, the *bcl-2* transgene allows cells to survive following STI571 treatment (20). Then, we assayed SE joining within a chromosomally integrated V(D)J recombination substrate (pMX-DEL-SJ) via a Southern blotting with

A

Age	$XLF^{\Delta/\Delta}DNA\text{-}PKcs^{+/+}$	$XLF^{\Delta/\Delta}DNA\text{-}PKcs^{+/-}$	$XLF^{\Delta/\Delta}DNA\text{-}PKcs^{-/-}$	Total
P1	13	29	6	48
Expected P1	12	24	12	
P7	91	138	7	236
Expected P7	59	118	59	
E15.5	13	21	10	44
Expected E15.5	11	22	11	

	$XLF^{\Delta/\Delta}Artemis^{+/+}$	$XLF^{\Delta/\Delta}Artemis^{+/-}$	$XLF^{\Delta/\Delta}Artemis^{-/-}$	
P7	10	25	9	44
Expected P7	11	22	11	

B

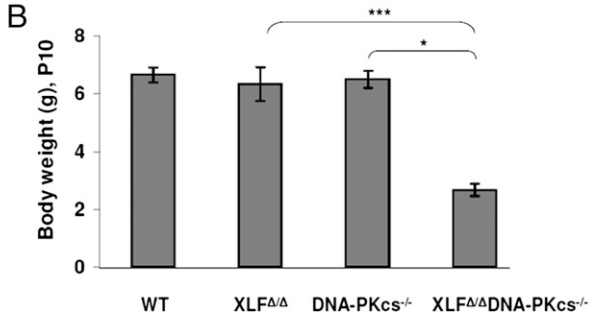

Fig. 1. Combined deficiency of DNA-PKcs and XLF significantly affects mouse growth and survival. (*A*) The number of live-born mice genotyped at day 1 (P1) or day 7 (P7), and number of mouse embryos at day E15.5, from crosses between $XLF^{\Delta/\Delta}DNA\text{-}PKcs^{+/-}$ mice are indicated (*Upper*). (*Lower*) The number of live-born mice (P7) from crosses between $XLF^{\Delta/\Delta}Artemis^{+/-}$ mice are indicated. (*B*) The body weight in grams of the indicated 10-d-old mice (P10) is plotted. The numbers represent the average and SD from at least 3 mice of each genotype. $*P = 0.01$ and $***P = 0.0003$.

which we can observe bands corresponding to the unrearranged cassette (UR), SEs, and SJs. (ref. 20; Fig. 2*A*).

Pro–B-cell lines from three different $XLF^{\Delta/\Delta}DNA\text{-}PKcs^{-/-}$ mice were tested, and all showed the same dramatic phenotype, compared with WT or single mutant lines, which was an accumulation of unjoined SEs consistent with nearly complete abrogation of SE joining (Fig. 2*B*). To test if this functional redundancy of DNA-PKcs involved its kinase activity, we treated both WT and $XLF^{\Delta/\Delta}$ v-Abl pro-B cells with DNA-PKcs–specific inhibitor Nu-7441. Upon STI571 treatment and RAG induction, the $XLF^{\Delta/\Delta}$ cells failed to join SEs, whereas vehicle-treated $XLF^{\Delta/\Delta}$ cells completed V(D)J recombination as efficiently as WT lines (Fig. 2*C*). Thus, DNA-PKcs kinase activity is required for efficient SE joining in $XLF^{\Delta/\Delta}$ cells. It is notable that the pro-B lines that were double deficient for XLF and Artemis ($XLF^{\Delta/\Delta}Artemis^{-/-}$) efficiently joined the SEs with very low levels of unjoined SEs consistent with the low levels observed in XLF-deficient cells alone (Fig. 2*D;* refs. 31, 32). Thus, the redundant functions of DNA-PKcs with XLF in SE joining rely on functions of the DNA-PKcs kinase separate from activation of Artemis.

DNA-PKcs and XLF Have Redundant Functions During CSR. We found that XLF and DNA-PKcs have redundant functions in SE joining during V(D)J recombination. To test whether inhibition of DNA-PKcs activity further impacts CSR in XLF-deficient cells, we activated WT or $XLF^{\Delta/\Delta}$ primary B cells for IgH CSR to IgG1 by culturing them in the presence of anti-CD40 plus IL-4, in the presence or absence of two different DNA-PKcs inhibitors (Nu-7026 and Nu-7441). In this context, treatment of WT-activated B cells had no significant effect on CSR to IgG1 in WT cells (Fig. 2*E* and Fig. S1), as previously observed (8). XLF-deficient B cells undergo CSR to IgG1 at about 30% the level of WT B cells at day 3,

GENETICS

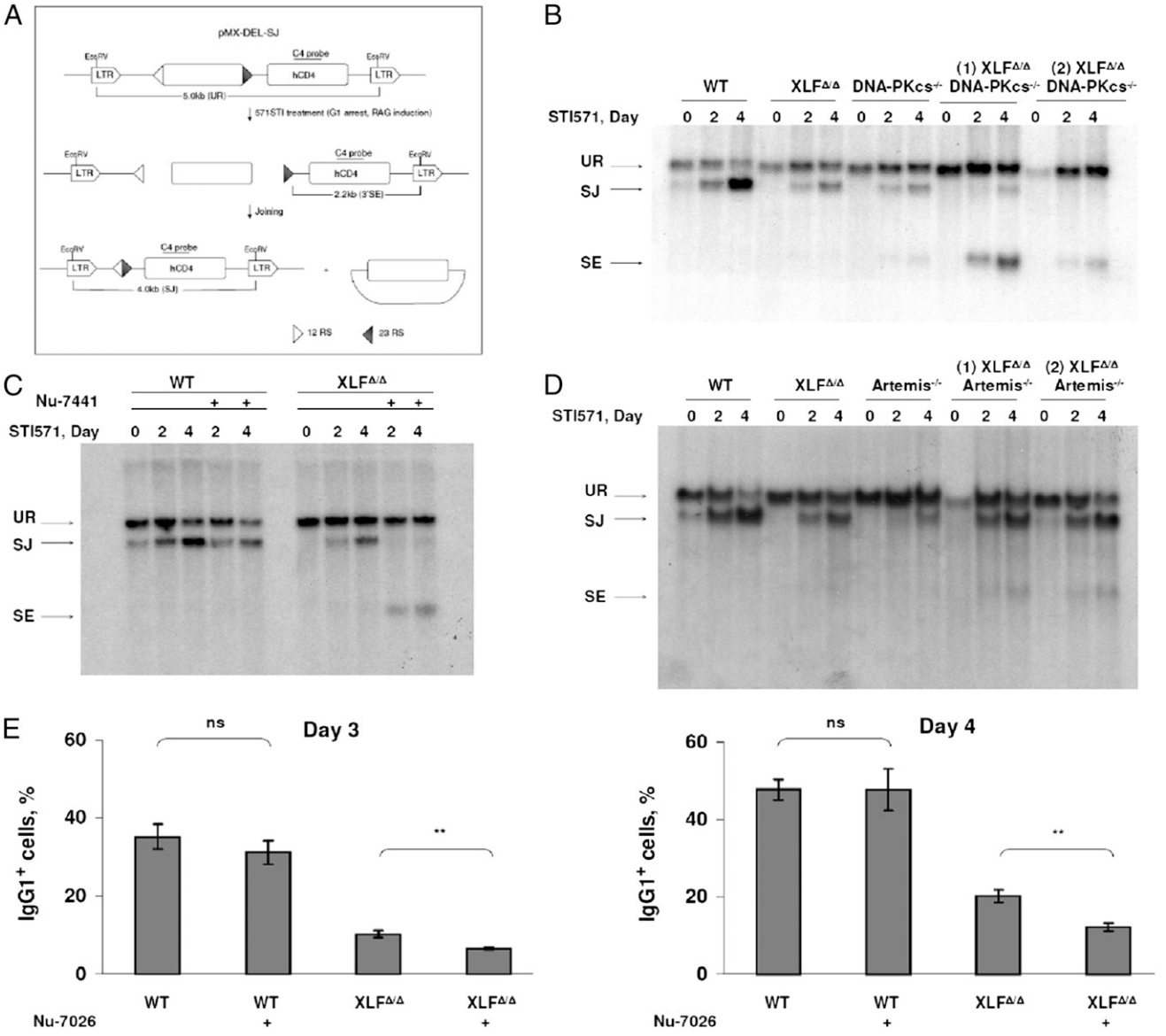

Fig. 2. XLF and DNA-PKcs have redundant functions for signal end joining and CSR. (*A*) Schematic diagram of chromosomally integrated V(D)J signal join cassette, pMX-DEL-SJ. (*B–D*) Southern blotting with C4 probe of DNA digested with EcoRV. The DNA was isolated from v-Abl pro–B-cell lines, with chromosomally integrated pMX-DEL-SJ cassettes, treated with STI571 for 2 or 4 d, and with DNA-PKcs inhibitor Nu-7441, when indicated. Detected bands are UR substrates, SJ, and SE. (*E*) IgG1 CSR levels of α-CD40/IL4-stimulated primary B cells (day 3 and day 4; $n = 5$ mice per genotype analyzed in independent experiments). Cell viability was not different between WT and XLF$^{\Delta/\Delta}$ stimulated B cells based on flow cytometric forward- and side-scatter profiles; DNA-PKcs inhibitor (Nu-7026) treatment also did not significantly affect cell viability, irrespective of genotype. Cell proliferation at day 3 (calculated as fold increase in starting cell number) (37), when proliferation is still robust, was not significantly affected by DNA-PKcs inhibitor: WT vs. WT + Nu-7026, $5.7^{+/-}$ 0.73 vs. $4.9^{+/-}$ 0.92, $P = 0.20$; XLF$^{\Delta/\Delta}$ vs. XLF$^{\Delta/\Delta}$ + Nu-7026, $5.9^{+/-}$1.43 vs. $4.7^{+/-}$ 1.57, $P = 0.25$; nor was it affected on day 4: WT vs. WT + Nu-7026, $7.8^{+/-}$ 3.41 vs. $8.1^{+/-}$ 2.99, $P = 0.86$; XLF$^{\Delta/\Delta}$ vs. XLF$^{\Delta/\Delta}$ + Nu-7026, $7.6^{+/-}$ 3.26 vs. $7.2^{+/-}$ 1.97, $P = 0.79$. Day 3 switching: $^{**}P = 0.0052$; n.s., not significant ($P = 0.39$). Day 4 switching: $^{**}P = 0.01$; n.s., not significant ($P = 0.74$), based on unpaired two-tailed *t* test. An independent set of CSR experiments using DNA-PKcs inhibitor Nu-7441 gave the same general results and is shown in Fig. S1.

and 40% the level of WT B cells at day 4. Treatment with DNA-PKcs inhibitors reduced levels to about 20% of WT at day 3, and 25% of WT at day 4, the latter of which is about the level of CSR observed via alternative end joining in the complete absence of C-NHEJ (Fig. 2*E*; refs. 31, 37). Therefore, XLF and DNA-PKcs appear to have redundant functions in CSR.

Unjoined RS Ends Are Not Excessively Resected in Absence of XLF. SEs and CEs are excessively resected in cells double deficient for XLF and histone H2AX, and to a lesser extent in cells deficient for XLF and ATM or XLF and 53BP1 (31, 32). Although XLF apparently does not prevent increased end resection in the combined absence of ATM or H2AX and either Artemis or Lig4 (34), ability of XLF to contribute to end protection through a different mechanism has not been tested. In this regard, we did not observe any evidence of increased resection of the unjoined SEs that accumulate in the absence of XLF and DNA-PKcs (Fig. 2 *B* and *C*; resection would be indicated by a "smear" or heterogeneous bands below the SE band as observed in refs. 31, 32, 34; see below). In a similar fashion, when we used the pMX-DEL-CJ V(D)J substrate to detect CEs and CJs in XLF$^{\Delta/\Delta}$DNA-PKcs$^{-/-}$ v-Abl pro–B-cell lines versus the various controls, we found no evidence of increased resection of unjoined CEs (Fig. 3 *A* and *B*; note the heterogeneous smear of bands below the CE band in XLF$^{\Delta/\Delta}$ cells treated with ATM inhibitor as positive control). In theory, lack of resection of unjoined CEs or SEs in the XLF/DNA-PKcs

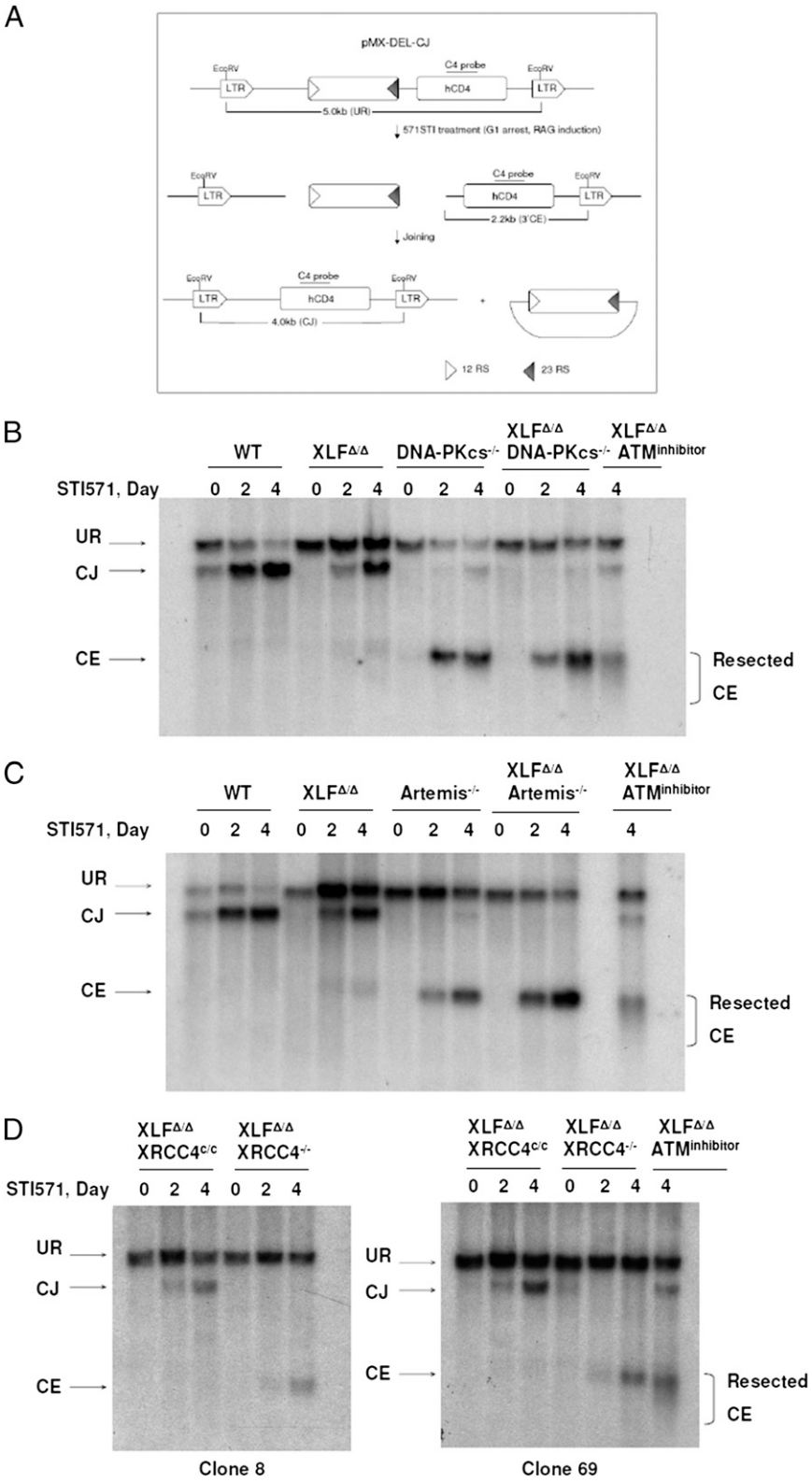

Fig. 3. Free CEs do not show increased resection in the absence of XLF. (*A*) Schematic diagram of chromosomally integrated V(D)J coding join cassette, pMX-DEL-CJ. (*B–D*) Southern blotting with C4 probe of DNA digested with EcoRV. The DNA was isolated from the indicated v-Abl pro–B-cell lines, with chromosomally integrated pMX-DEL-CJ cassettes, treated with STI571 for 2 or 4 d, and with ATM inhibitor Ku-55933, when indicated. Increased CE resection is indicated by the bracket labeled "resected CE" in the $XLF^{\Delta/\Delta}ATM^{inhibitor}$ lane.

double mutants might reflect some unknown role of DNA-PKcs, similar to that found for ATM (34), in activating resection. However, we also found no increased resection of unjoined CEs that accumulate in hairpin form in $XLF^{\Delta/\Delta}Artemis^{-/-}$ and as opened ends in $XLF^{\Delta/\Delta}XRCC4^{-/-}$ v-Abl transformed pro-B lines (Fig. 3 *C* and *D*). We conclude that, based on the resolution of currently available assays, XLF is not required for protection of free coding ends during V(D)J recombination.

XLF Has Redundant Functions with DNA-PKcs in Maintaining Genomic Stability. Combined deficiency for XLF and DNA-PKcs leads to a nearly complete block of SE joining in the V(D)J recombination

assay and to substantial inhibition of CSR to IgG1. To quantify potential effects on genome stability, we applied telomere fluorescence in situ hybridization (T-FISH) to quantify chromosome and chromatid breaks in tail fibroblasts from the various mouse lines. Levels of abnormal metaphases in XLF$^{\Delta/\Delta}$DNA-PKcs$^{-/-}$ fibroblasts (25.5%), were similar to those found in Ku70$^{-/-}$ cells (27.6%, $P = 0.69$), and significantly higher than in XLF$^{\Delta/\Delta}$ cells (12.0%, $P = 0.02$) or DNA-PKcs$^{-/-}$ cells (12.4%, $P = 0.01$), or wild type cells (3.6%, $P = 0.0004$) (Fig. 4*A*). Levels of chromosomal abnormalities in XLF$^{\Delta/\Delta}$Artemis$^{-/-}$ cells (12.0%) were similar to that of XLF$^{\Delta/\Delta}$ cells ($P = 1{,}0$), consistent with our finding that Artemis deficiency did not lead to increased defects in joining of V(D)J SEs in the absence of XLF (Fig. 2*D*). In XLF$^{\Delta/\Delta}$DNA-PKcs$^{-/-}$ fibroblasts, levels of chromosome breaks were much higher than those of chromatid breaks, indicating that, as observed for C-NHEJ–deficient lines previously (32, 38), most unrepaired DSB accumulated in pre-replicative phases of the cell cycle. We conclude that the XLF and DNA-PKcs also have redundant functions in promoting genomic stability.

Discussion

We find that XLF and DNA-PKcs functionally overlap in a variety of processes that rely on core C-NHEJ factors. Thus, RS joining during V(D)J recombination, which is known to be fully dependent on core C-NHEJ factors (1–4), occurs relatively normally in the absence of DNA-PKcs or XLF but is nearly abrogated in their combined absence (Fig. 2 *B* and *C*). Likewise, IgH CSR to IgG1 occurs normally in the absence of DNA-PKcs (5–7) or when DNA-PKcs kinase is inhibited (8), and at somewhat reduced efficiency in the absence of XLF (29); but CSR to IgG1 is further reduced to levels observed in the absence of core C-NHEJ factors in XLF-deficient cells treated with DNA-PKcs kinase inhibitors (Fig. 2*E* and Fig. S1). Spontaneous genomic instability, as assessed by analysis of metaphase karyotypes is only moderately affected by DNA-PKcs or XLF deficiency alone (9, 28, 32), but their combined deficiency increases levels to those found in cells deficient for a core C-NHEJ factor (Ku70) with primarily chromosome breaks as observed in cells with core C-NHEJ deficiencies (Fig. 4). Finally, DNA-PKcs or XLF deficiency do not greatly impact mouse development outside of the lymphoid system but combined deficiency leads to major growth defects and late prenatal or early postnatal lethality, reminiscent of some core C-NHEJ defects (Fig. 1). Together, these findings strongly indicate that XLF and DNA-PKcs provide redundant functions that are required for some aspects of the core C-NHEJ reaction.

Precisely how XLF and DNA-PKcs functionally overlap in C-NHEJ remains to be determined. Given that DNA-PKcs inhibitor treatment reveals the same functional XLF overlaps as DNA-PKcs deficiency where tested, one possibility is overlapping functions between XLF and DNA-PKcs substrates (Fig. 2 *B* and *C*). In this regard, Artemis and XLF do not have detectable overlapping functions in any tested process, which argues against the XLF overlapping function with DNA-PKcs involving currently known DNA-PKcs roles in end processing (Figs. 2D and 4A). Our findings also indicate that XLF is not required for end protection in DNA-PKcs or other C-NHEJ-factor–deficient cells, where ATM substrates H2AX and 53BP1 are present and known to function in that capacity (Figs. 2 B and C and 3). DNA-PKcs long has been suggested to have direct roles in end synapsis and potential roles for DNA-PKcs substrates are conceivable. ATM and its substrates also have been suggested to function in DSB synapsis (20, 39). It is notable that combined deficiency for ATM and DNA-PKcs leads to decreased RS joining (16, 23), but not nearly to the extent found in the absence of either ATM or DNA-PKcs and XLF (ref. 31 and Fig. 2 *B* and *C*). Thus, XLF has functional redundancy with both proteins that cannot be compensated by either DNA-PKcs or ATM alone. Such a function may be through directly overlapping roles in the same process or through roles in very different processes that functionally overlap (31). For example, all three proteins might contribute directly to synapsis, or, alternatively, DNA-PKcs and ATM might contribute to synapsis, and XLF could recruit repair factors to enhance the kinetics with which C-NHEJ ligates ends before they separate. Many other possible direct or

A

Spontaneous genomic instability in tail fibroblasts

Genotype	Number of mice	Total Metaphases	Abnormal metaphases,		Chromosomal breaks	Chromatid breaks
		n	n	%	n	n
Wild type	5	250	9	3.6	13	1
XLF$^{\Delta/\Delta}$	5	250	30	12.0	39	7
DNA-PKcs$^{-/-}$	5	250	31	12.4	38	7
XLF$^{\Delta/\Delta}$DNA-PKcs$^{-/-}$	4	200	51	25.5	80	4
Artemis$^{-/-}$	5	250	10	4.0	12	0
XLF$^{\Delta/\Delta}$Artemis$^{-/-}$	5	250	30	12.0	45	2
Ku70$^{-/-}$	5	250	69	27.6	83	15

B

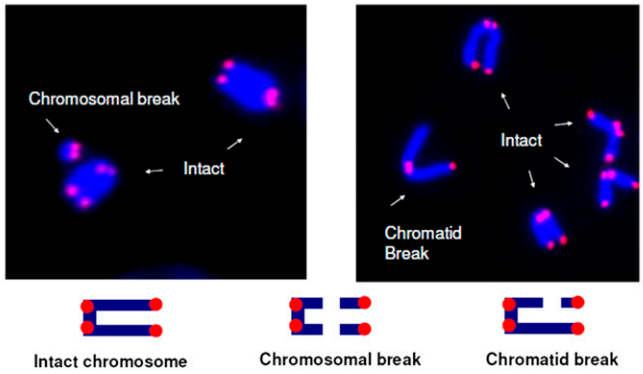

Fig. 4. Genomic instability in mice tail fibroblasts. (*A*) Telomere FISH analysis of metaphases from WT, XLF$^{\Delta/\Delta}$, DNA-PKcs$^{-/-}$, XLF$^{\Delta/\Delta}$DNA-PKcs$^{-/-}$, Artemis$^{-/-}$, XLF$^{\Delta/\Delta}$Artemis$^{-/-}$, and Ku70$^{-/-}$ fibroblasts. 200–250 total metaphases from four or five different mice, respectively, of each indicated genotype were analyzed. Numbers of different types of metaphase anomalies are indicated. (*B*) Examples of intact and abnormal chromosomes, including chromosome and chromatid breaks. Telomeres are in red (Cy3), and DNA is in blue (DAPI).

indirect functionally redundant roles could be imagined in the context of proposed overlapping activities of ATM and DNA-PKcs (8, 16, 23). Whatever their redundant functions with XLF, DNA-PKcs and ATM have distinct roles, as neither can substitute for XLF in the absence of the other.

Materials and Methods

Mice. All experiments involving mice were performed according to protocols approved by the Animal Resources Care Facility of Boston Children's Hospital (ARCH). Artemis$^{+/-}$ (40), DNA-PKcs$^{+/-}$ (15), Eμ-Bcl2^{+} (41), Ku70$^{+/-}$ (42), XLF$^{+/\Delta}$ (29), and XRCC4$^{C/+}$ (43) mice were previously described.

Chromosomal V(D)J Recombination Assays. V(D)J recombination with an integrated substrate was previously described (20, 31, 32). Where indicated, the cells were treated with 15 μM of ATM inhibitor Ku-55933 (Tocris Bioscience) or 5 μM of Nu-7441 DNA-PKcs inhibitor (Tocris Bioscience). XLF$^{\Delta/\Delta}$XRCC4$^{C/C}$ v-Abl clones with independent V(D)J cassette single integrations were treated with Tat-Cre and screened for *Xrcc4*$^{-/-}$ subclones as described (31, 44).

Class Switch Recombination Assay. Assays for IgH class switch recombination to IgG1 were carried out as previously described (37). In brief, mature B cells were isolated and pretreated with either DMSO vehicle or 5 μM of Nu-7026, or 5 μM of Nu-7441 (Tocris) and stimulated with anti-CD40 plus IL-4 . Cells were assessed for switching to IgG1 by fluorescence activated cell sorting on day 4 as described.

Primary Murine Tail Fibroblasts. Primary tail fibroblasts were generated as described (32). In brief, skin from mouse tail was removed and cut with blade to obtain pieces of about 2 mm × 2 mm. The skin pieces were treated 24 h with 2 mg/mL collagenase II (Gibco) in DMEM supplemented with 10% (vol/vol) heat-inactivated FCS and antibiotics, at 37 °C, 5% (vol/vol) CO_2 incubator. Then, the skin pieces were homogenized in 10-mL pipette by moving up and down, and filtered through a 70-μm nylon cell strainer (BD Falcon). Subsequently, the cells were washed in DMEM with 10% (vol/vol) FCS, and plated. Fibroblasts from the second or third passages were used for the telomere FISH assay.

Telomere FISH Assay. Metaphases were prepared and chromosomal aberrations were counted as described (32). The mouse tail fibroblasts were treated with 100 ng/mL colcemid (KaryoMax, Gibco) for 6 h. Then, the cells were treated with trypsin in PBS solution, washed with PBS, and lysed in 75 mM KCl (37 °C, 20 min). Subsequently, fibroblasts were fixed in methanol:acetic acid (3:1) as described (38). Telomeres were visualized with a Cy3-labeled $(CCCTAA)_3$ probe (Applied Biosystems), and DNA was visualized with DAPI. Images were obtained with Eclipse microscope (Nikon). Loss of telomere signal from both sister chromatids was defined as chromosomal break. Loss of telomere signal from one of the chromatids or clear absence of DAPI in the middle of one chromatid was defined as chromatid break.

ACKNOWLEDGMENTS. This work is supported by National Institutes of Health (NIH) Grant AI076210 (to F.W.A.) and NIH/National Cancer Institute Grant NCI 5R01CA158073 (to S.Z). B.S. is supported by the National Institute of Aging/NIH under Award K01 AG043630. F.W.A. is an investigator of the Howard Hughes Medical Institute. C.G. is a fellow of Cancer Research Institute.

1. Boboila C, Alt FW, Schwer B (2012) Classical and alternative end-joining pathways for repair of lymphocyte-specific and general DNA double-strand breaks. *Adv Immunol* 116:1–49.
2. Zhang Y, et al. (2010) The role of mechanistic factors in promoting chromosomal translocations found in lymphoid and other cancers. *Adv Immunol* 106:93–133.
3. Lieber MR, Ma Y, Pannicke U, Schwarz K (2004) The mechanism of vertebrate non-homologous DNA end joining and its role in V(D)J recombination. *DNA Repair (Amsterdam, Neth)* 3(8–9):817–826.
4. Bednarski JJ, Sleckman BP (2012) Lymphocyte development: Integration of DNA damage response signaling. *Adv Immunol* 116:175–204.
5. Manis JP, Dudley D, Kaylor L, Alt FW (2002) IgH class switch recombination to IgG1 in DNA-PKcs-deficient B cells. *Immunity* 16(4):607–617.
6. Jolly CJ, Cook AJ, Manis JP (2008) Fixing DNA breaks during class switch recombination. *J Exp Med* 205(3):509–513.
7. Bosma GC, et al. (2002) DNA-dependent protein kinase activity is not required for immunoglobulin class switching. *J Exp Med* 196(11):1483–1495.
8. Callén E, et al. (2009) Essential role for DNA-PKcs in DNA double-strand break repair and apoptosis in ATM-deficient lymphocytes. *Mol Cell* 34(3):285–297.
9. Franco S, et al. (2008) DNA-PKcs and Artemis function in the end-joining phase of immunoglobulin heavy chain class switch recombination. *J Exp Med* 205(3):557–564.
10. Lieber MR, et al. (1988) The defect in murine severe combined immune deficiency: Joining of signal sequences but not coding segments in V(D)J recombination. *Cell* 55(1):7–16.
11. Malynn BA, et al. (1988) The scid defect affects the final step of the immunoglobulin VDJ recombinase mechanism. *Cell* 54(4):453–460.
12. Blackwell TK, et al. (1989) Isolation of scid pre-B cells that rearrange kappa light chain genes: Formation of normal signal and abnormal coding joins. *EMBO J* 8(3):735–742.
13. Taccioli GE, et al. (1998) Targeted disruption of the catalytic subunit of the DNA-PK gene in mice confers severe combined immunodeficiency and radiosensitivity. *Immunity* 9(3):355–366.
14. Kurimasa A, et al. (1999) Catalytic subunit of DNA-dependent protein kinase: Impact on lymphocyte development and tumorigenesis. *Proc Natl Acad Sci USA* 96(4): 1403–1408.
15. Gao Y, et al. (1998) A targeted DNA-PKcs-null mutation reveals DNA-PK-independent functions for KU in V(D)J recombination. *Immunity* 9(3):367–376.
16. Zha S, et al. (2011) Ataxia telangiectasia-mutated protein and DNA-dependent protein kinase have complementary V(D)J recombination functions. *Proc Natl Acad Sci USA* 108(5):2028–2033.
17. Fukumura R, et al. (1998) Murine cell line SX9 bearing a mutation in the dna-pkcs gene exhibits aberrant V(D)J recombination not only in the coding joint but also in the signal joint. *J Biol Chem* 273(21):13058–13064.
18. Errami A, et al. (1998) XR-C1, a new CHO cell mutant which is defective in DNA-PKcs, is impaired in both V(D)J coding and signal joint formation. *Nucleic Acids Res* 26(13): 3146–3153.
19. Fukumura R, et al. (2000) Signal joint formation is also impaired in DNA-dependent protein kinase catalytic subunit knockout cells. *J Immunol* 165(7):3883–3889.
20. Bredemeyer AL, et al. (2006) ATM stabilizes DNA double-strand-break complexes during V(D)J recombination. *Nature* 442(7101):466–470.
21. Sekiguchi J, et al. (2001) Genetic interactions between ATM and the nonhomologous end-joining factors in genomic stability and development. *Proc Natl Acad Sci USA* 98(6):3243–3248.
22. Gurley KE, Kemp CJ (2001) Synthetic lethality between mutation in Atm and DNA-PK (cs) during murine embryogenesis. *Curr Biol* 11(3):191-194.
23. Gapud EJ, et al. (2011) Ataxia telangiectasia mutated (Atm) and DNA-PKcs kinases have overlapping activities during chromosomal signal joint formation. *Proc Natl Acad Sci USA* 108(5):2022–2027.
24. Yano K, et al. (2008) Ku recruits XLF to DNA double-strand breaks. *EMBO Rep* 9(1):91–96.
25. Ahnesorg P, Smith P, Jackson SP (2006) XLF interacts with the XRCC4-DNA ligase IV complex to promote DNA nonhomologous end-joining. *Cell* 124(2):301–313.
26. Buck D, et al. (2006) Cernunnos, a novel nonhomologous end-joining factor, is mutated in human immunodeficiency with microcephaly. *Cell* 124(2):287–299.
27. Du L, et al. (2012) Cernunnos influences human immunoglobulin class switch recombination and may be associated with B cell lymphomagenesis. *J Exp Med* 209(2):291–305.
28. Zha S, Alt FW, Cheng HL, Brush JW, Li G (2007) Defective DNA repair and increased genomic instability in Cernunnos-XLF-deficient murine ES cells. *Proc Natl Acad Sci USA* 104(11):4518–4523.
29. Li G, et al. (2008) Lymphocyte-specific compensation for XLF/cernunnos end-joining functions in V(D)J recombination. *Mol Cell* 31(5):631–640.
30. Vera G, et al. (2012) Cernunnos deficiency reduces thymocyte lifespan and alters the T cell repertoire in mice and humans. *Mol Cell Biol*, 10.1128/MCB.01057-12.
31. Zha S, et al. (2011) ATM damage response and XLF repair factor are functionally redundant in joining DNA breaks. *Nature* 469(7329):250–254.
32. Oksenych V, et al. (2012) Functional redundancy between repair factor XLF and damage response mediator 53BP1 in V(D)J recombination and DNA repair. *Proc Natl Acad Sci USA* 109(7):2455–2460.
33. Liu X, et al. (2012) Overlapping functions between XLF repair protein and 53BP1 DNA damage response factor in end joining and lymphocyte development. *Proc Natl Acad Sci USA* 109(10):3903–3908.
34. Helmink BA, et al. (2011) H2AX prevents CtIP-mediated DNA end resection and aberrant repair in G1-phase lymphocytes. *Nature* 469(7329):245–249.
35. Bothmer A, et al. (2010) 53BP1 regulates DNA resection and the choice between classical and alternative end joining during class switch recombination. *J Exp Med* 207(4):855–865.
36. Bunting SF, et al. (2010) 53BP1 inhibits homologous recombination in Brca1-deficient cells by blocking resection of DNA breaks. *Cell* 141(2):243–254.
37. Yan CT, et al. (2007) IgH class switching and translocations use a robust non-classical end-joining pathway. *Nature* 449(7161):478–482.
38. Franco S, et al. (2006) H2AX prevents DNA breaks from progressing to chromosome breaks and translocations. *Mol Cell* 21(2):201–214.
39. Bassing CH, Alt FW (2004) H2AX may function as an anchor to hold broken chromosomal DNA ends in close proximity. *Cell Cycle* 3(2):149–153.
40. Rooney S, et al. (2002) Leaky Scid phenotype associated with defective V(D)J coding end processing in Artemis-deficient mice. *Mol Cell* 10(6):1379–1390.
41. Strasser A, Harris AW, Cory S (1991) bcl-2 transgene inhibits T cell death and perturbs thymic self-censorship. *Cell* 67(5):889–899.
42. Gu Y, et al. (1997) Growth retardation and leaky SCID phenotype of Ku70-deficient mice. *Immunity* 7(5):653–665.
43. Yan CT, et al. (2006) XRCC4 suppresses medulloblastomas with recurrent translocations in p53-deficient mice. *Proc Natl Acad Sci USA* 103(19):7378–7383.
44. Boboila C, et al. (2012) Robust chromosomal DNA repair via alternative end joining in the absence of X-ray repair cross-complementing protein 1 (XRCC1). *Proc Natl Acad Sci USA* 109(7):2473–2478.